

Differential cross sections for the electron-impact excitation of He-like ions: 2^3S and 2^3P

Yukikazu Itikawa and Kazuhiro Sakimoto

Institute of Space and Astronautical Science, Yoshinodai, Sagamihara-shi 229, Japan

(Received 1 February 1988)

Differential cross sections for the electron-impact excitation of ions are calculated and compared along the He-like isoelectronic sequence. With the use of a distorted-wave method, cross sections are obtained for the transitions $1^1S \rightarrow 2^3S, 2^3P$ in $\text{Li}^+, \text{O}^{6+}$, and Si^{12+} . A comparison is also made to the cases of neutral He and the limit $Z \rightarrow \infty$ (Z being the nuclear charge). When scaled by multiplication by Z^4 and compared at the same energy in threshold units, the resulting cross sections are quite similar both in magnitude and in angular distribution all along the isoelectronic sequence. The Coulomb-wave approximation is also used to calculate the differential cross section to test its validity.

I. INTRODUCTION

In the study of electron collisions with neutral atoms and molecules, it is customary to calculate differential cross sections (DCS) when a comparison is made between theory and experiment or between different theories. In the case of electron-ion collisions, however, a very limited number of papers have reported DCS so far. It is very hard to obtain DCS experimentally for electron-ion collisions, though a few attempts have already been made.¹ This lack of experimental data has discouraged any theoretical calculation of DCS for electron-ion collisions. The DCS is valuable in getting insight into the physical mechanism of the collision process. Furthermore, differences in theoretical approximations can be easily seen in the DCS. Taking account of these points, the present authors have started a systematic study of DCS for electron-impact excitations of atomic ions.

In the present paper excitation cross sections are calculated with the use of the distorted-wave-exchange-approximation method recently developed by Itikawa and Sakimoto (called the DWXA).² This method is rather simple and easily adapted to a systematic study. It has been applied to the calculation of (integrated) cross sections for the excitation of He-, Be-, and C-like ions.^{2,3} The resulting cross sections have been found reasonably accurate except near threshold. For comparison, the Coulomb-wave approximation is also used here to calculate the DCS in some cases.

As the first step of our study, He-like ions are chosen. In particular, the DCS for the excitation of 2^3S and 2^3P states are calculated and compared along the isoelectronic sequence of He. The comparison includes two extreme cases: neutral He and the limit $Z \rightarrow \infty$ (Z being the nuclear charge). To facilitate the comparison of different ions, a scaling is proposed in the expression of the cross section and the collision energy.

In Sec. II the formulas for the calculation of the DCS are given. The formulas are a rather straightforward extension of those for neutral atoms, but they are shown in somewhat detail because of the lack of any detailed re-

port on the DCS for ions. In Sec. III calculations are made for the excitation of 2^3S and 2^3P states of several He-like ions and the results are compared to each other and to the extreme cases of neutral He and the limit $Z \rightarrow \infty$. Some discussions and concluding remarks are given in Sec. IV. For the convenience of the reader, details of the calculation of the DCS in the limit $Z \rightarrow \infty$ are described in Appendix.

II. THE FORMULAS OF THE DIFFERENTIAL CROSS SECTION

Details of the present distorted-wave method (DWXA) are given in a previous paper.² It is based on the following assumptions.

- (1) Introducing a distortion potential U^{DW} and regarding the difference between the true interaction and U^{DW} as a perturbation, we adopt the standard theory of first-order perturbation to derive the transition probability.
- (2) In the actual calculation, U^{DW} is taken to be a spherical average of the electrostatic potential formed by the target ion in its initial state.
- (3) The same distortion potential is used both for the initial and for the final states.
- (4) Electron exchange is taken into account only between the two interacting electrons. The possibility of the ejection of the third electron is ignored.

The differential cross section for the excitation $\alpha \rightarrow \beta$ is given by

$$\frac{d\sigma}{d\omega}(\alpha \rightarrow \beta) = \frac{1}{4\pi^2} \frac{k_\beta}{k_\alpha} |T_{\beta\alpha}|^2. \quad (2.1)$$

Here k_α (k_β) is the wave number of the incident (scattered) electron and $T_{\beta\alpha}$ is the respective element of the transition matrix. Atomic units are used throughout this paper, unless otherwise stated. The detailed form of $T_{\beta\alpha}$ is given in a previous paper.² In the present calculation, we assume the LS scheme of the angular momentum coupling. After averaging over the initial direction of the (spin and orbital) angular momenta of the target and summing over the final direction of those, we have

$$\begin{aligned}
\frac{d\sigma}{d\omega}(\alpha L^\alpha S^\alpha \rightarrow \beta L^\beta S^\beta) &= \frac{k_\beta}{k_\alpha} \frac{2}{(2L^\alpha+1)(2S^\alpha+1)} \\
&\times \sum_S (2S+1) \sum_L \sum_{\bar{L}} \sum_l \sum_{\bar{l}} \sum_{l'} \sum_{\bar{l}'} \sum_\nu P_\nu(\cos\theta) i^{l-l'-\bar{l}+\bar{l}'} (-1)^{-L^\alpha+L^\beta} \\
&\times (2L+1)(2\bar{L}+1)(2\nu+1) \\
&\times [(2l+1)(2\bar{l}+1)(2l'+1)(2\bar{l}'+1)]^{1/2} \\
&\times \begin{Bmatrix} l & \bar{l} & \nu \\ 0 & 0 & 0 \end{Bmatrix} \begin{Bmatrix} l' & \bar{l}' & \nu \\ 0 & 0 & 0 \end{Bmatrix} \begin{Bmatrix} \nu & \bar{l} & l \\ L^\alpha & L & \bar{L} \end{Bmatrix} \begin{Bmatrix} \nu & \bar{l}' & l' \\ L^\beta & L & \bar{L} \end{Bmatrix} \\
&\times \exp[i(\eta_l^{(\alpha)} + \eta_{l'}^{(\beta)} - \eta_{\bar{l}}^{(\alpha)} - \eta_{\bar{l}'}^{(\beta)})] \\
&\times (\langle T^{(d)} \rangle_{\beta\alpha} + \langle T^{(ex)} \rangle_{\beta\alpha}) (\langle \bar{T}^{(d)} \rangle_{\beta\alpha} + \langle \bar{T}^{(ex)} \rangle_{\beta\alpha})^*. \quad (2.2)
\end{aligned}$$

Here $L^\alpha S^\alpha$ ($L^\beta S^\beta$) are the orbital and spin angular momenta of the initial (final) states of the target ion, P_ν is the Legendre function, θ is the scattering angle of the colliding electron, and $\eta_l^{(s)}$ is the phase shift of the distorted wave of the electron (having an angular momentum l) scattered in the target of state s ($=\alpha$ or β). The reduced transition matrix elements, $\langle T^{(d)} \rangle_{\beta\alpha}$ and $\langle T^{(ex)} \rangle_{\beta\alpha}$, are presented in a previous paper.² The barred ones, $\langle \bar{T}^{(d)} \rangle_{\beta\alpha}$ and $\langle \bar{T}^{(ex)} \rangle_{\beta\alpha}$, are obtained by replacing l, l', L with $\bar{l}, \bar{l}', \bar{L}$ in the expression for $\langle T^{(d)} \rangle_{\beta\alpha}$ and $\langle T^{(ex)} \rangle_{\beta\alpha}$.

Quite often in the case of electron-ion collisions, the Coulomb phase is treated separately. We divide the phase $\eta_l^{(s)}$ into two parts:

$$\eta_l^{(s)} = \delta_l^{(s)} + \rho_l^{(s)}, \quad (2.3)$$

where $\rho_l^{(s)}$ is the corresponding Coulomb phase

$$\rho_l^{(s)} = \arg \Gamma \left[l + 1 - i \frac{q}{k_s} \right]. \quad (2.4)$$

Here the distortion potential has been assumed to have an asymptotic form

$$U^{DW} \sim -\frac{q}{r} \text{ as } r \rightarrow \infty. \quad (2.5)$$

Now we introduce another quantity derived from the T matrix elements:

$$\begin{aligned}
T_{ll'}^{LS}(\alpha \rightarrow \beta) &= 4\sqrt{k_\alpha k_\beta} \exp[i(\delta_l^{(\alpha)} + \delta_{l'}^{(\beta)})] \\
&\times (\langle T^{(d)} \rangle_{\beta\alpha} + \langle T^{(ex)} \rangle_{\beta\alpha}). \quad (2.6)
\end{aligned}$$

Then Eq. (2.2) can be rewritten in the form

$$\frac{d\sigma}{d\omega}(\alpha L^\alpha S^\alpha \rightarrow \beta L^\beta S^\beta) = \sum_{\nu=0}^{\infty} A_\nu(\alpha \rightarrow \beta) P_\nu(\cos\theta) \quad (2.7)$$

with

$$\begin{aligned}
A_\nu(\alpha \rightarrow \beta) &= \frac{1}{8k_\alpha^2} \frac{1}{(2L^\alpha+1)(2S^\alpha+1)} \sum_S (2S+1) \sum_L \sum_{\bar{L}} \sum_l \sum_{\bar{l}} \sum_{l'} \sum_{\bar{l}'} \sum_\nu (-1)^{-L^\alpha+L^\beta} Z(l\bar{l}\bar{L}; L^\alpha \nu) Z(l'\bar{l}'\bar{L}; L^\beta \nu) \\
&\times \exp[i(\rho_l^{(\alpha)} + \rho_{l'}^{(\beta)} - \rho_{\bar{l}}^{(\alpha)} - \rho_{\bar{l}'}^{(\beta)})] \\
&\times T_{ll'}^{LS}(\alpha \rightarrow \beta) T_{\bar{l}\bar{l}'}^{\bar{L}S}(\alpha \rightarrow \beta)^*. \quad (2.8)
\end{aligned}$$

The coefficient Z is defined in terms of the 3- j and 6- j symbols as

$$Z(abcd; ef) = i^{f-a+c} (-1)^{b+d} [(2a+1)(2b+1)(2c+1)(2d+1)(2f+1)]^{1/2} \begin{Bmatrix} a & c & f \\ 0 & 0 & 0 \end{Bmatrix} \begin{Bmatrix} f & c & a \\ e & b & d \end{Bmatrix}. \quad (2.9)$$

When we introduce an angular momentum transfer j , the formula (2.8) can be expressed in the form

$$A_\nu(\alpha \rightarrow \beta) = \frac{1}{8k_\alpha^2} \frac{1}{(2L^\alpha+1)(2S^\alpha+1)} \sum_S (2S+1) \sum_l \sum_{\bar{l}} \sum_{l'} \sum_{\bar{l}'} \sum_j X(l\bar{l}\bar{l}'j\nu) T_j^{ll'}(\alpha \rightarrow \beta) T_j^{\bar{l}\bar{l}'}(\alpha \rightarrow \beta)^*, \quad (2.10)$$

where

$$X(l\bar{l}\bar{l}'j\nu) = i^{l-l'+\bar{l}-\bar{l}'} (-1)^{j+\nu} (2j+1)(2\nu+1) \begin{Bmatrix} l & \bar{l} & \nu \\ 0 & 0 & 0 \end{Bmatrix} \begin{Bmatrix} l' & \bar{l}' & \nu \\ 0 & 0 & 0 \end{Bmatrix} \begin{Bmatrix} l & \bar{l} & \nu \\ \bar{l}' & l' & j \end{Bmatrix} \quad (2.11)$$

and

$$T_j^{ll'}(\alpha \rightarrow \beta) = \sum_L (-1)^L (2L+1) [(2l+1)(2l'+1)]^{1/2} (-1)^{-l-l'-L\alpha-L\beta} \begin{Bmatrix} l & L^\alpha & L \\ L^\beta & l' & j \end{Bmatrix} \exp[i(\rho_l^{(\alpha)} + \rho_{l'}^{(\beta)})] T_{ll'}^{LS}(\alpha \rightarrow \beta). \quad (2.12)$$

The expression (2.10) completely coincides with the corresponding one given by Salvini.⁴ For the numerical calculation of DCS, we employ Salvini's computer code with $T_{ll'}^{LS}$ in Eq. (2.6). The latter T matrix elements are obtained in the same way as in a previous paper.² (The original Salvini's code has been found to contain some errors. The corrected version is used in the present calculation.)

III. He-LIKE IONS

The previous work on He-like ions² is now extended to the calculation of DCS. As in a previous study, the target state is represented by a configuration-interaction-type wave function produced by the CIV3 code.⁵

As the first step of the systematic study of DCS, the transitions $1^1S \rightarrow 2^3S, 2^3P$ of He-like ions are considered here. It should be noted that the convergence of the partial-wave expansion is slower for the DCS than for the integrated cross section. The contribution of higher partial waves has to be more carefully treated in the DCS calculation. For the spin forbidden transitions such as $1^1S \rightarrow 2^3S, 2^3P$, however, the transition matrix elements decrease rapidly with increasing angular momentum of the incident electron. For those transitions, therefore, the convergence problem is much less severe. The result of the study of spin-allowed transitions will be reported in another paper after a critical test of the convergence.

In the following, we compare cross sections for ions with different nuclear charge Z , along the He isoelectronic sequence. In the case of H-like ions, Burgess, Hummer, and Tully⁶ show that the cross section multiplied by Z^4 varies slowly with Z when compared as a function of the scaled collision energy E/Z^2 . Here, scaled differential cross sections $Z^4 d\sigma/d\omega$, are plotted against scattering angles at a given electron energy in threshold units, $X (=E/\Delta E, \Delta E$ being the threshold energy).

A. 2^3S

Figures 1-3 show the DCS for Li^+ , O^{6+} , and Si^{12+} calculated at $X=1.2, 2.0$, and 2.7 , respectively. In the present case, the T matrix elements are calculated for $L \leq 19$ and the partial-wave expansion is well converged. Our scaling over Z is so successful that the resulting values of the DCS fit in the same scale. Furthermore the angular dependence of the DCS for the three ions are very similar, except for Li^+ at $X=1.2$. In particular, the scaled DCS for O^{6+} almost coincides with that for Si^{12+} both in magnitude and in angular dependence.

To complete the comparison along the isoelectronic sequence, two extreme cases are also shown in the figures: neutral He ($Z=2$) and the limit $Z \rightarrow \infty$. There are a large number of calculations of DCS reported for He. To make the comparison meaningful, we have chosen the result of the calculation based on the method similar to ours (i.e., DWXA). Figures 2 and 3 show the (scaled) DCS for He calculated by Thomas *et al.*⁷ at $X=2.03$ and 2.78 (i.e., $E=40$ and 55 eV, respectively). They used the first-order many-body theory, which is essentially the same as our DWXA (see the review by Itikawa⁸). Very interestingly, the DCS for He has an angular dependence qualitatively similar to those for the ions. This indicates that the mechanism of the excitation process in the ions is not much different from that for the neutral atom, at least at those collision energies.

Near threshold ($X \sim 1$) it is very difficult to obtain reliable cross sections for neutral He with the use of any distorted-wave method. No data for He, therefore, are shown in Fig. 1. For ions, particularly for highly-charged ions, a distorted-wave method can give accurate cross sections even near threshold.⁸ The DCS given in Fig. 1 are expected to represent real ones, at least to some

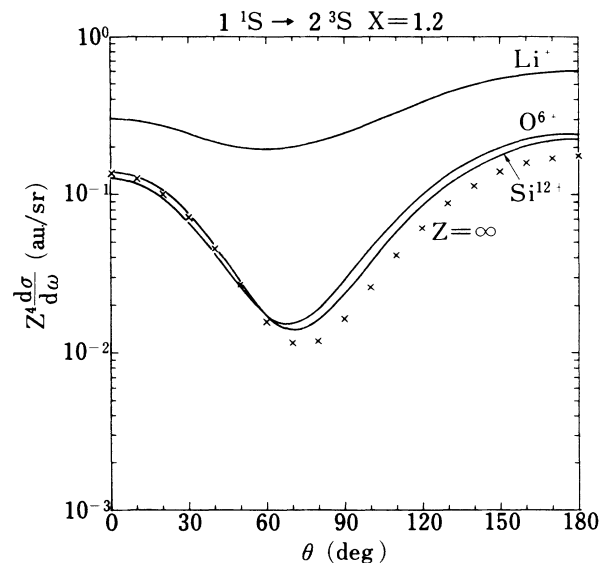


FIG. 1. The scaled differential cross section, $Z^4 d\sigma/d\omega$ (in a.u./sr), for the excitation $1^1S \rightarrow 2^3S$ of the He-like ions: Li^+ , O^{6+} , Si^{12+} . The values in the limit $Z \rightarrow \infty$ are also shown. The calculation was made at $X=1.2$ (X being the collision energy in threshold units) with the use of the DWXA.

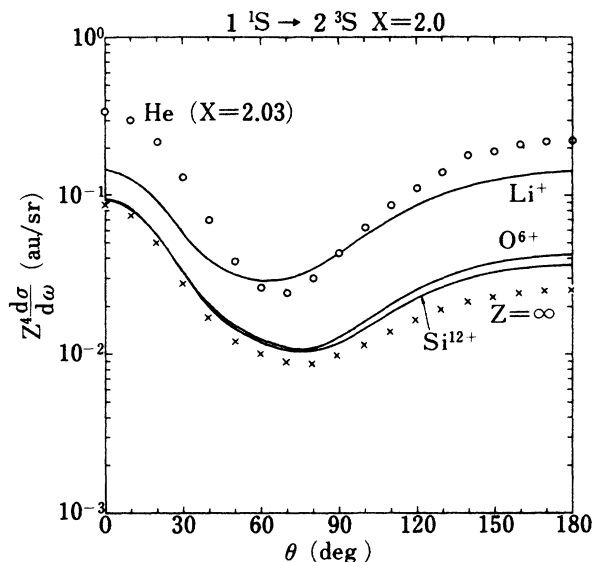


FIG. 2. Same as in Fig. 1, but for the energy $X=2.0$. Open circles are the corresponding differential cross sections for He calculated by Thomas *et al.*⁷ at $X=2.03$.

extent. It should be noted, however, that the present DW method does not take into account any resonance effects which may distort the DCS near threshold.

Figures 1–3 show also the DCS in the limit $Z \rightarrow \infty$. The method of the calculation in the limit is described in Appendix. Briefly, the limiting value is obtained in the Coulomb-wave approximation with a hydrogenic target function. (Note that no relativistic effects are considered here.) As is seen in the figures, the (scaled) DCS for O^{6+} and Si^{12+} are very close to the limiting value. A detailed

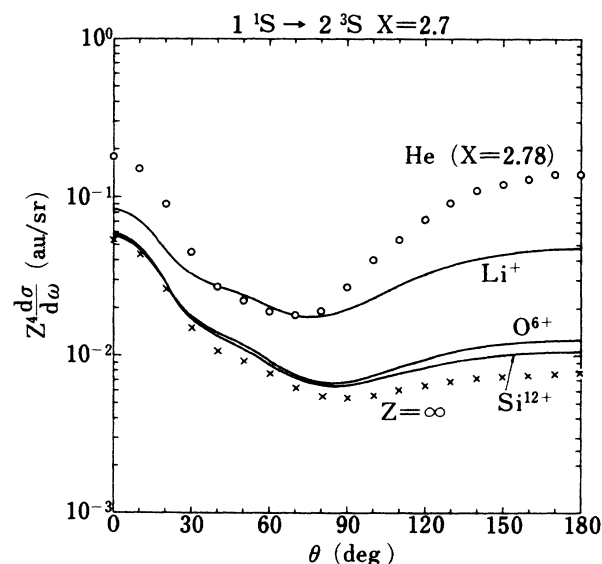


FIG. 3. Same as in Fig. 1, but for the energy $X=2.7$. Cross sections for He (calculated by Thomas *et al.*⁷ at $X=2.78$) are also shown.

comparison, however, shows that the convergence along Z is not uniform. In Figs. 2 and 3, for instance, the DCS near $\theta=0^\circ$ for O^{6+} is a little closer to the corresponding limit than that for Si^{12+} . This may be ascribed to the variation in the target wave functions, which are optimized independently for each ion in the present calculation.

From Figs. 1–3 one can see the general trend of the DCS as a function of electron energy (X). With increasing X , the angular dependence of the scaled DCS for the three ions are getting closer to each other. This means that the interaction between the incident electron and the target nucleus dominates in the collision at the higher energy.

As an example of a comparison of DCS obtained by different theories, Fig. 4 shows the cross section calculated in the Coulomb-wave approximation at $X=2.0$. In this approximation (called CBXA in a previous paper²), the distorted wave of the electron is replaced by the corresponding Coulomb wave. The value for $Z = \infty$ in Fig. 4, therefore, is exactly the same as that in Fig. 2. From a comparison between Figs. 2 and 4, we can conclude that the DCS (CBXA) for Li^+ is very different from the DCS (DWXA) but, for O^{6+} and Si^{12+} , there is much less difference between the two calculations. In the case of the integrated cross section,² the CBXA gives too large an absolute value for Li^+ in the region $X \leq 5$, but the energy dependence of the cross section is the same for the CBXA and the DWXA. Figure 4, however, clearly shows that the CBXA result for Li^+ is completely different from the DWXA calculation at $X=2.0$. A preliminary calculation shows that this discrepancy of the DCS for Li^+ persists at least up to $X=3.0$.

B. 2^3P

Figure 5 gives the DCS calculated for the excitation of 2^3P state of Li^+ , O^{6+} , and Si^{12+} . As in Fig. 2, the two

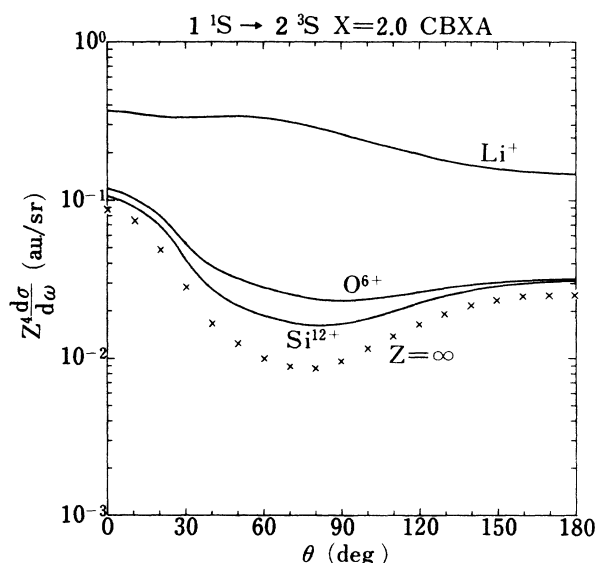


FIG. 4. Same as in Fig. 1, but the values obtained by the Coulomb-wave approximation (CBXA) at $X=2.0$.

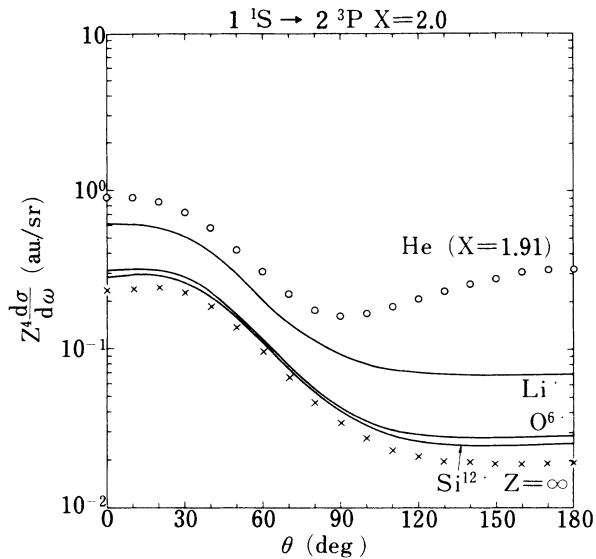


FIG. 5. The scaled differential cross section, $Z^4 d\sigma/d\omega$ (in a.u./sr), for the excitation $1^1S \rightarrow 2^3P$ of the He-like ions: Li^+ , O^{6+} , Si^{12+} . The values in the limit $Z \rightarrow \infty$ are also shown. The calculation was made at $X=2.0$ with the use of the DWXA. Cross sections for He (calculated by Thomas *et al.*⁷ at $X=1.91$) are plotted for comparison.

extreme cases (i.e., $Z=2$ and ∞) of the isoelectronic sequence are also presented in Fig. 5. All of those cross sections have been calculated at $X=2.0$.

The overall feature of the DCS for 2^3P along the isoelectronic sequence is quite similar to that for 2^3S . In particular, as in Figs. 1–3, the (scaled) cross section of O^{6+} is almost equal to that of Si^{12+} and both of them are very close to the one in the limit $Z \rightarrow \infty$.

For the transition $1^1S \rightarrow 2^3P$ to occur, the electrons pass the target at a distance because of the necessity of angular-momentum exchange. In other words, the partial waves with nonzero angular momentum dominates in the transition. On the other hand, the s wave has the largest contribution to the excitation $1^1S \rightarrow 2^3S$. This difference can explain the different behavior of the DCS at large angles for the excitations of 2^3P and 2^3S . That is, the s -wave contribution increases the DCS at large angles for the excitation of 2^3S . In the case of 2^3P excitation of He, the enhancement of the backward scattering is attributed probably to the strong short-range electrostatic interaction.

The dominance of the higher partial waves in the excitation of the 2^3P state leads to the fact that the Coulomb-wave approximation may be good in that case. Figure 6 shows the result of the Coulomb-wave calculation (CBXA). When compared to the case of 2^3S excitation, the CBXA gives qualitatively good results even for Li^+ . The absolute magnitude of the DCS for Li^+ , however, still largely differs from the corresponding value obtained in the DWXA calculation.

IV. DISCUSSION AND CONCLUSION

As is mentioned in the introduction, very few papers have been published on the calculation of the DCS for

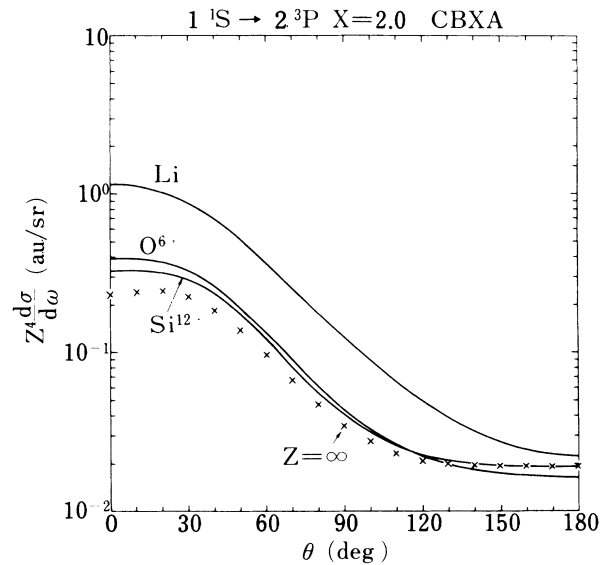


FIG. 6. Same as in Fig. 5, but the values obtained by the Coulomb-wave approximation (CBXA).

the electron-impact excitation of He-like ions. Only the paper by Bhatia and Temkin⁹ gives the DCS for the excitation of 2^3S and 2^3P states which can be compared to the present result. Their calculation is based on the “one-sided” approximation of the distorted-wave method. They take into account a distortion in the initial state, while the Coulomb wave is used for the scattered electron in the final state. Furthermore their target wave function is very simple when compared to that in the present calculation. [McDowell *et al.*¹⁰ made a calculation of the (integrated) cross section for He-like ions with the use of a similar distorted-wave method. They compared the target wave function of Bhatia and Temkin to a more accurate one and concluded that the former wave function gives different results from those of the latter. It would be of interest to study the dependence of the DCS on the target wave function, but it will be a future task.] As a result, the DCS for the excitation of 2^3S of Li^+ calculated by Bhatia and Temkin are completely different from those reported in the present paper. (Bhatia and Temkin reported no DCS for the 2^3S excitation of other ions.) Because the one-sided approximation is known to be generally unreliable,⁸ no detailed comparison is made here between the result of Bhatia and Temkin and ours. It should be noted, however, that our DCS for the 2^3P excitation has much resemblance to that of Bhatia and Temkin. This is another manifestation of the fact that higher partial waves dominate in the $1^1S \rightarrow 2^3P$ transition.

In the present paper, a systematic study of the DCS for the excitations of 2^3S and 2^3P states is made along the isoelectronic sequence of He-like ions. When the scaled cross sections (i.e., $Z^4 d\sigma/d\omega$) are compared at the same electron energy in threshold units, they are similar in shape and magnitude to each other. In particular, the cross sections for O^{6+} and Si^{12+} are close to the limiting value at $Z = \infty$. In other words, the scaled cross section

in the limit $Z \rightarrow \infty$ can be used to approximate the DCS for the highly charged ions.

A detailed comparison of the DCS can make clear the validity of the theoretical approximations used to obtain them. In the present paper, the Coulomb-wave approximation (CBXA) is compared to the DWXA. For the process $1^1S \rightarrow 2^3S$, the CBXA result for Li^+ is completely different from the corresponding DWXA one. In the case of 2^3P excitation of Li^+ , the two calculations are qualitatively similar, but of much difference in magnitude. There is much less disagreement between the two calculations for the DCS of O^{6+} and Si^{12+} . This kind of comparison would be of interest if extended to any other theoretical methods.

No experimental data are available at present to be compared to the present result of DCS. A few attempts of the energy loss measurement in electron-ion collisions are now under way. Hopefully in the future the present result will be scrutinized by experiment.

APPENDIX: CROSS SECTIONS IN THE LIMIT $Z \rightarrow \infty$

In the target system with $Z \gg N$ (N being the number of bound electrons), the electron-electron interaction can be ignored in comparison to the electron-nucleus one. The target wave function for that system becomes a simple product of N hydrogenic eigenfunctions with the nuclear charge Z . Furthermore, when $Z \gg N$, the electrostatic potential of the target ion is reduced to the potential formed by the target nucleus. Thus the distorted wave of the incident electron in this case is obtained as a Coulomb function for charge Z , which is orthogonal to the one-particle function of the bound state of the target.

The cross section formula in the limit $Z \rightarrow \infty$ was studied in detail by Sampson.¹¹ He showed that, in the limit $Z \rightarrow \infty$, the reactance matrix element of He-like ions, R_{He} , can be expressed in terms of those for H-like ions, R_{H} . For the transition

$$e + \text{He-like} (1s^2 L^\alpha = 0, S^\alpha = 0) \rightarrow e + \text{He-like} (1s2l^\beta L^\beta S^\beta),$$

we have, according to Sampson

$$R_{\text{He}}^{(d)} = \sqrt{2} R_{\text{H}}^{(d)} (1s \rightarrow 2l^\beta) \delta_{L\beta l^\beta} \delta_{S\beta 0}, \quad (\text{A1})$$

$$R_{\text{He}}^{(\text{ex})} = \sqrt{2} R_{\text{H}}^{(\text{ex})} (1s \rightarrow 2l^\beta) \delta_{L\beta l^\beta} G(S^\beta, S), \quad (\text{A2})$$

with

$$G(S^\beta, S) = \frac{1}{2} \text{ for } S^\beta = 0 \ (S = \frac{1}{2}), \quad (\text{A3})$$

$$= -\sqrt{3}/2 \text{ for } S^\beta = 1 \ (S = \frac{1}{2}). \quad (\text{A4})$$

Here the superscripts (d) and (ex) indicate, respectively, the direct and the exchange parts of the matrix element. For the H-like ions with $Z = \infty$, the reactance matrix element can be easily obtained as

$$Z R_{\text{H}}^{(d)}(\alpha \rightarrow \beta) = 2 \int \int d\mathbf{r}_1 d\mathbf{r}_2 \xi_l^{(\beta)}(\mathbf{r}_1) \phi_\beta(\mathbf{r}_2)^* (1/r_{12}) \times \xi_l^{(\alpha)}(\mathbf{r}_1) \phi_\alpha(\mathbf{r}_2), \quad (\text{A5})$$

$$Z R_{\text{H}}^{(\text{ex})}(\alpha \rightarrow \beta) = 2 \int \int d\mathbf{r}_1 d\mathbf{r}_2 \xi_l^{(\beta)}(\mathbf{r}_1) \phi_\beta(\mathbf{r}_2)^* (1/r_{12}) \times \xi_l^{(\alpha)}(\mathbf{r}_2) \phi_\alpha(\mathbf{r}_1), \quad (\text{A6})$$

where ϕ_s and $\xi_l^{(s)}$ ($s = \alpha$ or β) are, respectively, the bound state and the continuum eigenfunction of the one-particle Hamiltonian

$$h(\mathbf{r}) = -\frac{1}{2} \nabla^2 - \frac{1}{r}. \quad (\text{A7})$$

The radial part of $\xi_l^{(s)}$ is normalized to have an asymptotic form

$$\xi_l^{(s)} \sim k_s^{-1/2} \sin \left[k_s r + \frac{1}{k_s} \ln(2k_s r) - \frac{\pi}{2} l + \rho_l^{(s)} \right] \text{ as } r \rightarrow \infty, \quad (\text{A8})$$

where $\rho_l^{(s)}$ is the Coulomb phase shift with $q=1$ [see Eq. (2.4)].

The transition matrix $\langle T \rangle_{\beta\alpha}$ introduced in the previous paper² is related to the above reactance matrix as follows:

$$\langle T^{(d)} \rangle_{\beta\alpha} = -\frac{1}{2\sqrt{k_\alpha k_\beta}} R^{(d)}(\alpha \rightarrow \beta), \quad (\text{A9})$$

$$\langle T^{(\text{ex})} \rangle_{\beta\alpha} = \frac{1}{2\sqrt{k_\alpha k_\beta}} R^{(\text{ex})}(\alpha \rightarrow \beta). \quad (\text{A10})$$

Burgess, Hummer, and Tully⁶ calculated $Z R_{\text{H}}^{(d)}$ and $Z R_{\text{H}}^{(\text{ex})}$ for $1s \rightarrow 2s, 2p$ transitions in the H-like ion with $Z = \infty$. Inserting those values of $R_{\text{H}}^{(d)}$ and $R_{\text{H}}^{(\text{ex})}$ into (A1) and (A2) and using the relations (A9) and (A10), we can easily get the transition matrix elements for the $1s^2 \rightarrow 1s2s, 1s2p$ transitions in the He-like ion with $Z = \infty$. The resulting matrix elements are incorporated into the formulas in Sec. III to give the DCS in the limit $Z \rightarrow \infty$.

¹For example, I. D. Williams, A. Chutjian, and R. J. Mawhorter, J. Phys. B **19**, 2189 (1986).

²Y. Itikawa and K. Sakimoto, Phys. Rev. A **31**, 1319 (1985).

³Y. Itikawa and K. Sakimoto, Phys. Rev. A **33**, 2320 (1986).

⁴S. A. Salvini, Comput. Phys. Commun. **27**, 25 (1982).

⁵A. Hibbert, Comput. Phys. Commun. **9**, 141 (1975).

⁶A. Burgess, D. G. Hummer, and J. A. Tully, Philos. Trans. R. Soc. London, Ser. A **A266**, 225 (1970).

⁷L. D. Thomas, Gy. Csanak, H. S. Taylor, and B. S. Yarlagadda, J. Phys. B **7**, 1719 (1974).

⁸Y. Itikawa, Phys. Rep. **143**, 69 (1986).

⁹A. K. Bhatia and A. Temkin, J. Phys. B **10**, 2893 (1977).

¹⁰M. R. C. McDowell, L. A. Morgan, V. P. Myerscough, and T. Scott, J. Phys. B **10**, 2727 (1977).

¹¹D. H. Sampson, Astrophys. J. Suppl. Ser. **28**, 309 (1974).